BER Prediction using EXIT Charts for BICM with Iterative Decoding

Thorsten Clevorn, Susanne Godtmann, and Peter Vary

***Abstract*— A method for the prediction of bit-error rates (BER) of bit-interleaved coded modulation systems with iterative decoding (BICM-ID) is presented, which is based solely upon the extrinsic information transfer (EXIT) chart and avoids extensive BER simulations. Comparisons show an accurate prediction, even for low BERs down to 10^{-6}. Furthermore, an easy procedure to obtain the optimum rotation angle for a signal constellation set in conjunction with IQ Interleaving is described. Both methods can be applied to all types of channels.**

***Index Terms*— BICM-ID, EXIT chart, BER, IQ interleaving.**

I. Introduction

BIT-INTERLEAVED coded modulation with iterative decoding (BICM-ID) [1] is a bandwidth efficient coded modulation scheme which increases the time-diversity and consequently is especially suited for Rayleigh fading channels. At the receiver the channel decoder and the demodulator exchange extrinsic information in a Turbo process. Such Turbo processes are often analyzed using extrinsic information transfer (EXIT) charts [2]. In [2] also a method is presented to predict the BER of a Turbo code system using only the EXIT chart.

We extend this method to BICM-ID. This extension is not straightforward, because for BICM-ID no information on the data bits is available in the EXIT chart itself. Using the proposed method extensive BER simulations can be avoided. Comparisons with such simulations demonstrate that the BERs can be very accurately predicted in the whole E_b/N_0-range, even for much lower BERs (down to 10^{-6}) than in [2].

Additionally, using elements of this algorithm we demonstrate how to obtain the optimum rotation angle in case of IQ interleaving for a signal constellation set. These methods are both applicable to all types of channels for which the respective EXIT chart can be generated and are not limited to the exemplary Rayleigh fading channel.

II. The BICM-ID System

The considered BICM-ID transmitter encodes a block of data bits u by a standard non-systematic feed-forward convolutional encoder. The resulting encoded bits x are permuted by a pseudo-random bit-interleaver π to $\tilde{x}$ and grouped consecutively into bit patterns $\underline{\tilde{x}}_t = [\tilde{x}_t^{(1)}, \ldots \tilde{x}_t^{(I)}]$, where $\tilde{x}_t^{(i)}$ denotes the i^{th} bit in the bit pattern at time index t, $t = 1, \ldots T$. I is the number of bits that will be mapped to one channel symbol later on, e.g., $I = 3$ in case of 8PSK. The modulator maps an interleaved bit pattern $\underline{\tilde{x}}_t$ according to a mapping μ to a complex channel symbol y_t out of the signal constellation set (SCS) $\mathcal{Y}$. Note, to achieve a noticeable iterative gain other mappings than Gray mapping have to be used [1],[3],[4].

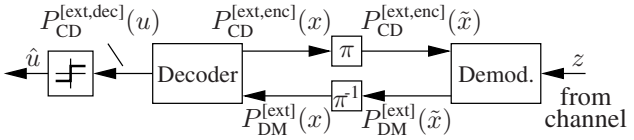

Fig. 1. Baseband model of the BICM-ID receiver.

The channel symbols are normalized here to an average energy of $E_s = E\{\|y_t\|^2\} = 1$. As exemplary channel model we use the memoryless Rayleigh channel. The transmitted symbols y_t are faded by the Rayleigh distributed coefficients a_t with $E\{\|a_t\|^2\} = 1$. In this paper we assume perfect knowledge of the channel state information. Next, complex zero-mean white Gaussian noise $n_t = n_t' + jn_t''$ with a known power spectral density of $\sigma_n^2 = N_0$ ($\sigma_{n'}^2 = \sigma_{n''}^2 = N_0/2$) is added. Thus, the received symbols z_t can be written as $z_t = a_t y_t + n_t$.

Fig. 1 depicts the baseband model of the BICM-ID receiver, which evaluates the received symbols z in a Turbo process. The demodulator (DM) computes extrinsic probabilities $P_{\text{DM}}^{[\text{ext}]}(\tilde{x})$ for each bit $\tilde{x}_t^{(i)}$ being $b \in \{0,1\}$ according to [1]

$$P_{\text{DM}}^{[\text{ext}]}(\tilde{x}_t^{(i)} = b) \sim \sum_{\hat{y} \in \mathcal{Y}_b^i} P(z_t|\hat{y}) \prod_{j=1, j\neq i}^{I} P_{\text{CD}}^{[\text{ext,enc}]}\left(\tilde{x}_t^{(j)} = \mu^{-1}(\hat{y})^{(j)}\right) \quad (1)$$

Each $P_{\text{DM}}^{[\text{ext}]}(\tilde{x})$ consists of the sum over all possible channel symbols $\hat{y}$ for which the i^{th} bit of the corresponding bit pattern $\underline{\tilde{x}} = \mu^{-1}(\hat{y})$ is b. These channel symbols form the subset $\mathcal{Y}_b^i$ with $\mathcal{Y}_b^i = \{\mu([\tilde{x}^{(1)}, \ldots \tilde{x}^{(I)}]) | \tilde{x}^{(i)} = b\}$. In the first iteration the feedback probabilities $P_{\text{CD}}^{[\text{ext}]}(\tilde{x})$ are initialized as equiprobable, i.e., $P_{\text{CD}}^{[\text{ext}]}(\tilde{x}) = 0.5$. The conditional probability density $P(z_t|\hat{y}) = (1/\pi\sigma_n^2)\exp(-d_{z\hat{y}}^2/\sigma_n^2)$ with $d_{z\hat{y}}^2 = \|z_t - a_t\hat{y}\|^2$ describes the complex channel.

After appropriately deinterleaving the $P_{\text{DM}}^{[\text{ext}]}(\tilde{x})$ to $P_{\text{DM}}^{[\text{ext}]}(x)$, the $P_{\text{DM}}^{[\text{ext}]}(x)$ are fed into a Soft-Input Soft-Output (SISO) channel decoder (CD), which computes extrinsic probabilities $P_{\text{CD}}^{[\text{ext}]}(x_t^{(i)})$ for the encoded bits $x_t^{(i)} = \{0,1\}$ in addition to the preliminary estimated decoded data bits $\hat{u}$. For the next iteration the $P_{\text{CD}}^{[\text{ext}]}(x)$ are interleaved again to $P_{\text{CD}}^{[\text{ext}]}(\tilde{x})$ in order to be fed into the demodulator. Note, in all steps of the receiver L-values (log-likelihood ratios) can be used instead of probabilities $P(\cdot)$ [1].

Manuscript received June 28, 2005. The associate editor coordinating the review of this letter and approving it for publication was Prof. Giorgio Taricco. This work was supported by the DFG (Deutsche Forschungsgemeinschaft).

The authors have been with the Institute of Communication Systems and Data Processing, RWTH Aachen University, Germany (e-mail: clevorn@ind.rwth-aachen.de). S. Godtmann is now with the Institute for Integrated Signal Processing Systems, RWTH Aachen University, Germany.

Digital Object Identifier 10.1109/LCOMM.2006.01012.

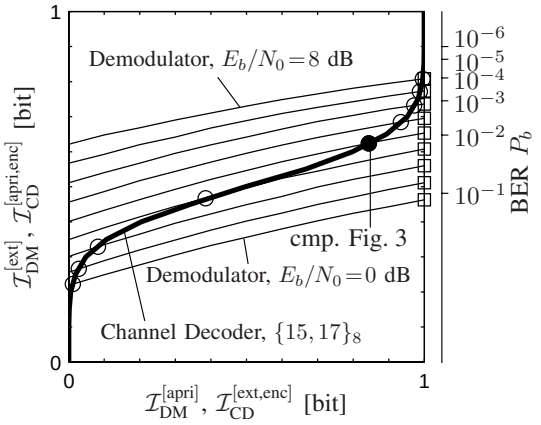

Fig. 2. EXIT characteristics for 8PSK-SP, Rayleigh channel.

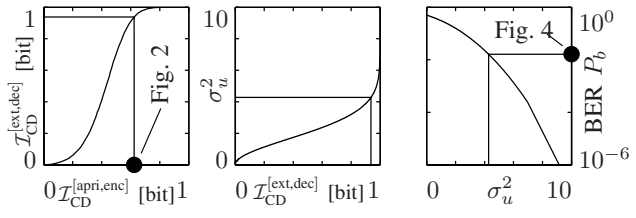

Fig. 3. The steps for BER prediction ("●" example for 8PSK-SP at 4 dB).

III. BER Prediction using EXIT Charts

EXIT charts [2],[5] are a powerful tool to analyze and optimize the convergence behavior of iterative systems utilizing the Turbo principle, i.e., systems exchanging and refining extrinsic information. The capabilities of the components, in our case the demodulator (DM) and the channel decoder (CD), are analyzed separately. The extrinsic mutual information $\mathcal{I}^{[\mathrm{ext}]}$ obtained by each component for a certain a priori mutual information $\mathcal{I}^{[\mathrm{apri}]}$ is determined. Both, $\mathcal{I}^{[\mathrm{ext}]}$ and $\mathcal{I}^{[\mathrm{apri}]}$, are calculated on the basis of the actual bits, e.g., x, and the available information, extrinsic or a priori, for these bits. As basis for this calculation usually histograms of the respective L-values, e.g., $L_{\mathrm{DM}}^{[\mathrm{ext}]}$ of $P_{\mathrm{DM}}^{[\mathrm{ext}]}$ for $\mathcal{I}_{\mathrm{DM}}^{[\mathrm{ext}]}$, are used. For the EXIT characteristics the a priori L-values are simulated as uncorrelated Gaussian distributed, with variance σ_A^2 and mean $\mu_A = \sigma_A^2/2$. The convergence behavior of BICM-ID has been studied, e.g., in [6],[7],[8].

In this letter, we extend the capabilities of the EXIT chart to the prediction of BERs P_b, as proposed for Turbo codes in [2] and, e.g., applied to iterative MIMO receivers in [5]. However, the adaptation is not straightforward because in contrast to [2] the mutual information on the data bits u, $\mathcal{I}_{\mathrm{CD}}^{[\mathrm{ext,dec}]}$, is not used in the EXIT chart, but the mutual information on the encoded bits x, $\mathcal{I}_{\mathrm{CD}}^{[\mathrm{ext,enc}]}$. In Fig. 2 the EXIT characteristics for an 8-state, rate-1/2, feed-forward convolutional code with generator polynomials $\{15, 17\}_8$ and for 8PSK-SP (set-partitioning) mapping [1] are depicted. The EXIT characteristic of the demodulator, $\mathcal{I}_{\mathrm{DM}}^{[\mathrm{ext}]} = f(\mathcal{I}_{\mathrm{DM}}^{[\mathrm{apri}]})$, depends on the channel quality, while the channel decoder characteristic, $\mathcal{I}_{\mathrm{CD}}^{[\mathrm{ext,enc}]} = f(\mathcal{I}_{\mathrm{CD}}^{[\mathrm{apri,enc}]})$, is independent of E_b/N_0, because the only input for the decoder is $P_{\mathrm{DM}}^{[\mathrm{ext}]}(x)$. Thus, also $\mathcal{I}_{\mathrm{CD}}^{[\mathrm{ext,dec}]}$, and consequently the BER P_b of the data bits u, depend solely on $\mathcal{I}_{\mathrm{CD}}^{[\mathrm{apri,enc}]} = \mathcal{I}_{\mathrm{DM}}^{[\mathrm{ext}]}$. The points "○" mark the intersections between the EXIT characteristics of demodulator and channel decoder and the points "□" mark the EXIT characteristics of the demodulator at $\mathcal{I}_{\mathrm{DM}}^{[\mathrm{apri}]} = 1$ bit (cmp. Fig. 4).

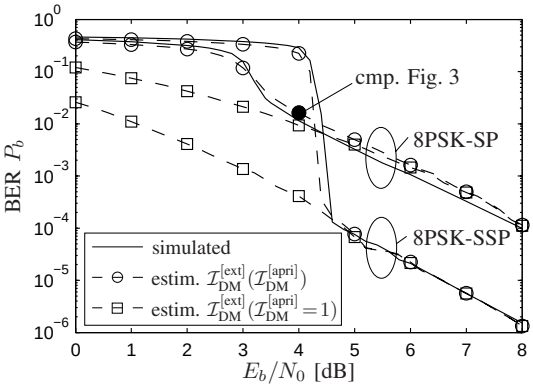

Fig. 4. Simulated and predicted BERs, 8-state conv. code, Rayleigh channel.

With the additionally measured EXIT characteristic $\mathcal{I}_{\mathrm{CD}}^{[\mathrm{ext,dec}]} = f(\mathcal{I}_{\mathrm{CD}}^{[\mathrm{apri,enc}]})$ for the decoded output of the decoder (Fig. 3, left plot) and the assumption of a Gaussian distributed decoder output $L_{\mathrm{CD}}^{[\mathrm{ext}]}(u)$ with variance σ_u^2 [2] we can stepwise calculate the BER. As example in Fig. 3 we use 8PSK-SP mapping at $E_b/N_0 = 4$ dB (point "●" in Figs. 2 and 4).

- Using the respective EXIT characteristic we can obtain $\mathcal{I}_{\mathrm{CD}}^{[\mathrm{ext,dec}]}$ for a given $\mathcal{I}_{\mathrm{CD}}^{[\mathrm{apri,enc}]} = \mathcal{I}_{\mathrm{DM}}^{[\mathrm{ext}]}$ (Fig. 3, left plot).
- With the inverse relation $\sigma_u \approx J^{-1}(\mathcal{I}_{\mathrm{CD}}^{[\mathrm{ext,dec}]})$ (this function cannot be expressed in closed form; for details see [2]) the variance σ_u^2 is computed (Fig. 3, center plot).
- Finally, the BER P_b is calculated as $P_b = \frac{1}{2}\,\mathrm{erfc}\left(\frac{\sigma_u^2}{2\sqrt{2}}\right)$ (Fig. 3, right plot)

On the right side of Fig. 2 a second axis for the BER is added. As already discussed before, the BER is independent of $\mathcal{I}_{\mathrm{CD}}^{[\mathrm{ext,enc}]} = \mathcal{I}_{\mathrm{DM}}^{[\mathrm{apri}]}$. Thus, in contrast to the systems in [2],[5], for the considered BICM-ID system the curves of constant BER are simply horizontal lines (not depicted in Fig. 2).

In Fig. 4 the predicted BERs are compared with simulated BERs for the 8-state convolutional code of Fig. 2 and 8PSK-SP and 8PSK-SSP (semi-set-partitioning) mappings [1]. The block size is 12000 data bits per frame and 30 iterations are performed at the receiver. For infinite block size, a perfect interleaver, and a sufficient number of iterations the decoding trajectory should reach the intersection of the channel decoder characteristic and the demodulator characteristic in the EXIT chart. In Fig. 2 these points are marked by "○" for the depicted characteristics. As visible in Fig. 4 the corresponding estimated BERs (dashed curve "○") quite well match the simulated BERs (solid curve) in the whole depicted E_b/N_0-range. The waterfall-region as well as the error floor are accurately predicted, providing a simple design tool for BICM-ID systems for all channel conditions.

A key feature for the analysis of BICM-ID is the error floor [1],[3],[4]. In [7],[4] it was shown that the error floor can be analyzed using the EXIT chart. For the analysis of the error floor, error-free feedback (EFF) for the demodulator is assumed (for details see, e.g., [1]). This EFF is similar to perfect a priori knowledge, i.e., $\mathcal{I}_{\mathrm{DM}}^{[\mathrm{apri}]} = 1$ bit. Thus, the asymptotic behavior, i.e., the error floor, can be analyzed using

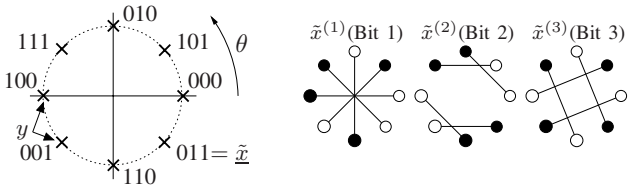

Fig. 5. 8PSK-SSP mapping [1] with EFF decision distances.

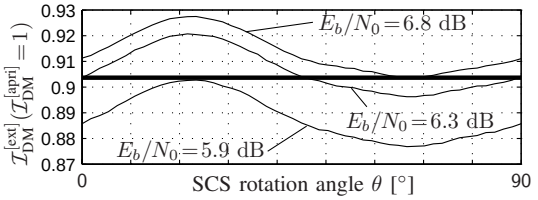

Fig. 6. $\mathcal{I}_{\mathrm{DM}}^{[\mathrm{ext}]}(\mathcal{I}_{\mathrm{DM}}^{[\mathrm{apri}]}=1)$ vs. rotation angle θ for 8PSK-SSP mapping.

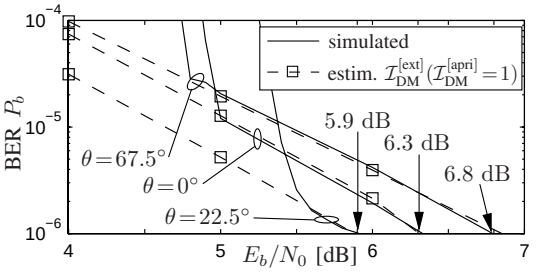

Fig. 7. Simulated and predicted BERs, 8-state conv. code, 8PSK-SSP, Rayleigh channel with IQ interleaving.

the right axis of the EXIT chart [7],[4]. Consequently, for estimation of the error floor of the BER we have to use the demodulator characteristics at $\mathcal{I}_{\mathrm{DM}}^{[\mathrm{apri}]}=1$ bit (points marked "□" in Fig. 2). Furthermore, a nice feature is that these points with $\mathcal{I}_{\mathrm{DM}}^{[\mathrm{apri}]}=1$ bit can also be evaluated numerically, see e.g. [7], instead of using extensive Monte-Carlo simulations. The respective curve for the BER in Fig. 4 (dashed curve marked "□") shows that also the asymptotic behavior alone is very well predicted. Comparing Figs. 2 and 4 reveals that the BER for 8PSK-SP reaches the error floor at $E_b/N_0\approx 4$ dB, corresponding to only $\mathcal{I}_{\mathrm{DM}}^{[\mathrm{apri}]}\approx 0.85$ bit, indicating that (in this case) already for $\mathcal{I}_{\mathrm{DM}}^{[\mathrm{apri}]}>0.85$ bit the feedback can be considered as quasi error-free.

The curves for 8PSK-SSP (see Fig. 5) in Fig. 4 demonstrate that the proposed BER estimation is accurate for BERs down to at least 10^{-6}. In contrast, the BER prediction for Turbo codes in [2] is only reliable for BERs down to 10^{-3}.

IV. Optimum Rotation Angles for IQ Interleaving

Using elements of the BER prediction method proposed in Section III we will in the following present a simple method for obtaining the optimum rotation angle θ for a mapping, when the signal space diversity [9] is exploited by IQ interleaving [10] for a Rayleigh channel. With separate interleaving of the in-phase (I) and quadrature (Q) component the performance is not anymore invariant to a rotation of the SCS [10]. Although IQ interleaving is especially suited for QAM SCSs, for consistency we consider exemplarily the 8PSK-SSP mapping [1] (Fig. 5) used before.

The error floor performance of BICM-ID is directly related to the decision distances for the EFF case, shown for 8PSK-SSP in Fig. 5 (right side). With IQ interleaving these distances shall not lie vertically or horizontally, but rather have large I and Q components. Examining the error floor we plot $\mathcal{I}_{\mathrm{DM}}^{[\mathrm{ext}]}(\mathcal{I}_{\mathrm{DM}}^{[\mathrm{apri}]}=1)$ for different rotation angles θ in Fig. 6. Note that, e.g., for the optimization of θ for non-iterative BICM you would use $\mathcal{I}_{\mathrm{DM}}^{[\mathrm{ext}]}(\mathcal{I}_{\mathrm{DM}}^{[\mathrm{apri}]}=0)$. As visible the highest $\mathcal{I}_{\mathrm{DM}}^{[\mathrm{ext}]}$ is obtained for $\theta=22.5°$, the lowest for $\theta=67.5°$. Intuitively, with $\theta=22.5°$ all distances for bits 1 and 2 have non-zero I and Q components and the distances for bit 3 even feature identical I and Q components resulting in a good performance. In contrast, for $\theta=67.5°$ the decision distances of bit 3 are parallel to the I or Q axis (I or Q component is zero), with bits 1 and 2 being principally similar to the $\theta=22.5°$ case.

With $\mathcal{I}_{\mathrm{CD}}^{[\mathrm{apri,enc}]}=\mathcal{I}_{\mathrm{DM}}^{[\mathrm{ext}]}$ the differences in required E_b/N_0 for a certain $\mathcal{I}_{\mathrm{DM}}^{[\mathrm{ext}]}$ are directly related to the BER as shown in Fig. 7. The mentioned E_b/N_0 correspond to a BER of 10^{-6}, i.e., $\mathcal{I}_{\mathrm{DM}}^{[\mathrm{ext}]}\approx 0.904$ in Fig. 6, for the respective rotation angle θ.

V. Conclusion

We presented a method to predict the BER of a BICM-ID system based solely on the EXIT characteristics of channel decoder and demodulator. Extensive BER simulations can be avoided. Comparisons show that the BERs of the waterfall and the error floor region are accurately estimated, even for relatively low BERs such as 10^{-6}. The error floor is already reached for an *a priori* mutual information lower than 1 bit. Furthermore, a procedure based on the EXIT chart to obtain the optimum rotation angle for an IQ interleaved signal constellation set is described. Both presented methods can be used in conjunction with all types of channels.

References

[1] X. Li, A. Chindapol, and J. A. Ritcey, "Bit-interleaved coded modulation with iterative decoding and 8PSK signaling," *IEEE Trans. Commun.*, vol. 50, pp. 1250–1257, Aug. 2002.

[2] S. ten Brink, "Convergence behavior of iteratively decoded parallel concatenated codes," *IEEE Trans. Commun.*, vol. 49, pp. 1727–1737, Oct. 2001.

[3] F. Schreckenbach, N. Görtz, J. Hagenauer, and G. Bauch, "Optimization of symbol mappings for bit-interleaved coded modulation with iterative decoding," *IEEE Commun. Lett.*, vol. 7, pp. 593–595, Dec. 2003.

[4] T. Clevorn, S. Godtmann, and P. Vary, "PSK versus QAM for iterative decoding of bit-interleaved coded modulation," in *Proc. IEEE Globecom*, vol. 1, Dec. 2004, pp. 341–345.

[5] E. Biglieri, A. Nordio, and G. Taricco, "Iterative receivers for coded MIMO signaling," *J. Wireless Commun. and Mobile Computing*, vol. 4, pp. 697–710, Nov. 2004.

[6] Y. Huang and J. A. Ritcey, "EXIT chart analysis of BICM-ID with imperfect channel state information," *IEEE Commun. Lett.*, vol. 7, pp. 434–436, Sept. 2003.

[7] T. Clevorn, S. Godtmann, and P. Vary, "EXIT chart analysis of non-regular signal constellation sets for BICM-ID," in *Proc. ISITA 2004*, Oct. 2004, pp. 21–26.

[8] J. Tan and G. L. Stüber, "Analysis and design of symbol mappers for iteratively decoded BICM," *IEEE Trans. Wireless Commun.*, vol. 3, pp. 662–672, Mar. 2005.

[9] J. Boutros and E. Viterbo, "Signal space diversity: a power- and bandwidth-efficient diversity technique for the Rayleigh fading channel," *IEEE Trans. Inform. Theory*, vol. 44, pp. 1453–1467, July 1998.

[10] A. Chindapol and J. A. Ritcey, "Design, analysis, and performance evaluation for BICM-ID with square QAM constellations in Rayleigh fading channels," *IEEE J. Select. Areas Commun.*, vol. 19, pp. 944–957, May 2001.